Backreaction effect and plasma oscillation in pair production for rapidly oscillating electric fields

R. Z. Jiang,[1,2] C. Gong,[3] Z. L. Li,[1,2,*] and Y. J. Li[1,2,†]

[1]*School of Science, China University of Mining and Technology, Beijing 100083, The People's Republic of China*
[2]*State Key Laboratory for GeoMechanics and Deep Underground Engineering, China University of Mining and Technology, Beijing 100083, The People's Republic of China*
[3]*North China Electric Power University, Baoding 071003, The People's Republic of China*

(Received 11 January 2023; accepted 29 September 2023; published 24 October 2023)

The backreaction effect and plasma oscillation in pair production for rapidly oscillating electric fields are investigated by solving the quantum Vlasov equation. It is found that the backreaction effect in the pair production is insignificant for a weak rapidly oscillating electric field regardless of whether the field has a frequency chirp or not. However, for a strong field, after the external field vanishes, there forms an obvious plasma oscillation. The oscillation period in some cases can be described by a simple formula constructed based on the Langmuir oscillation frequency, while in general, it depends directly on the parameters of the external field as well as the particle number density. Moreover, after considering the backreaction effect, the momentum spectrum presents irregular oscillations due to the development of a stochastic process in the dynamics of pair production. These findings give us a safety range of the external field parameters where the backreaction effect is negligible and deepen our understanding of the backreaction effect in the pair production for a rapidly oscillating field with or without a frequency chirp.

DOI: 10.1103/PhysRevD.108.076015

I. INTRODUCTION

Since Dirac proposed the relativistic wave equation and predicted the existence of positrons [1], much research has been done on how to produce electron-positron pairs from the vacuum. Sauter [2] solved the Dirac equation in the presence of a strong static electric field and found the level crossing of the positive and negative energy continuum, which indicates that electron-positron pairs can be produced by tunneling mechanism in the Dirac sea picture. And then, Schwinger [3] calculated the pair production rate in a constant field by the proper-time method in the framework of quantum electrodynamics and gave out the critical electric field strength $E_{\mathrm{cr}} = m^2/e \approx 1.3 \times 10^{18}\ \mathrm{V/m}$ (the natural units $\hbar = c = 1$ are used). As a result of these pioneering works, pair production from the vacuum in intense external fields is also known as the Sauter-Schwinger effect [4,5]. The laser intensity corresponding to the critical electric field strength is $I \approx 10^{29}\ \mathrm{W/cm^2}$, which is much larger than what current laser facilities can achieve [6–8], so it is not yet possible to produce observable electron pairs in experiments. However, with the rapid development of laser technology, many laser facilities are planning to achieve subcritical fields [9].

To reduce the threshold of pair production, several approaches have been proposed to produce observable electron pairs under subcritical electric field conditions. One method that can effectively enhance the pair production is the dynamically assisted Schwinger mechanism [10–14], in which the electric field adopts a combination of a strong slowly varying field and a weak rapidly oscillating one. Another approach is to use frequency chirp to increase the pair yield by increasing the effective frequency of the electric field. In Refs. [15–19], authors studied the effect of spatially homogeneous electric fields with frequency chirp on the pair production by the quantum kinetic equation and found that for some chirp parameters the pair yield could be improved 3 to 4 orders of magnitude. Moreover, the enhancement effect of pair production in a spatially inhomogeneous electric field with the frequency chirp was also studied [20,21].

It is known that electron-positron pairs produced from vacuum in a strong electric field can achieve a charge separation and form a new electric field; then this field in turn will affect the pair production [22–30]. This process is called the backreaction effect, and the new field is called the

[*]Corresponding author: zlli@cumtb.edu.cn
[†]Corresponding author: lyj@aphy.iphy.ac.cn

Published by the American Physical Society under the terms of the Creative Commons Attribution 4.0 International license. Further distribution of this work must maintain attribution to the author(s) and the published article's title, journal citation, and DOI. Funded by SCOAP[3].

internal electric field. For a subcritical external electric field, the number of produced particle pairs is relatively less, and the backreaction is generally ignored. However, when the subcritical electric field is modulated by a frequency chirp such as a linear chirp, a large number of particle pairs can be produced by absorbing some high-frequency photons and then be separated by the slowly varying part of the external field and form a strong internal electric field. Therefore, we think that the backreaction effect in this case is significant and cannot be neglected. In this paper, we will figure out the field parameter scope where the backreaction effect can be ignored for a rapidly oscillating electric fields and check whether the backreaction effect is negligible for a frequency chirped electric field.

In addition, when the backreaction effect is taken into account, a plasma oscillation may occur. In Ref. [24], the plasma oscillation in pair production for a sinusoidal electric field is studied by the quantum Vlasov equation (QVE), and an ultrarelativistic formula is given to estimate the oscillation period of the plasma. The ultrarelativistic formula shows that the oscillation period only depends on the maxima of the particle number density and has no direct relation to the field parameters. In this work, we will study the plasma oscillation for a rapidly oscillating electric field by QVE, explore the determining factors of the oscillation period, and check whether this formula still holds.

The structure of this paper is as follows: Sec. II briefly introduces the quantum kinetic theory including the backreaction effect. Section III is our numerical results: Sec. III A discusses the effect of the backreaction effect on the final particle number density; Sec. III B gives the effect of the backreaction effect on the momentum spectra; Sec. III C studies the factors affecting the plasma oscillation period; and Sec. III D checks the backreaction effect in pair production for a frequency chirped electric field. Section IV is a summary and discussion.

II. THEORETICAL FORMALISM

Since we focus on the backreaction effect in pair production for a rapidly oscillating electric field with or without a frequency chirp, the external field is simplified as a spatially homogeneous and time-dependent electric field. Of course, the spatial dependence of the external field including the magnetic field component should also be considered in practice [31–33]. Based on the study in Refs. [29,31–33] and the suppression effect of the spatial inhomogeneity on the pair production, we can speculate that in general the effect of the spatial inhomogeneity of the external field including the magnetic field component may play a role in weakening the backreaction effect. However, this study is beyond the scope of this paper and will be detailedly explored in future work. By using the temporal gauge, $A_0 = 0$, the spatially homogeneous and time-dependent four-vector potential can be written as $A_\mu = (0, 0, 0, A_{\rm ext}(t))$, and the external electric field is $E_{\rm ext} = -dA_{\rm ext}(t)/dt$. The form of the external electric field we used is

$$E_{\rm ext}(t) = E_0 \mathrm{e}^{-\frac{t^2}{2\tau^2}} \cos(\omega t + bt^2), \tag{1}$$

where E_0 is the amplitude of the electric field, ω is the unmodulated field frequency, τ is the pulse duration, and b denotes the chirp parameter.

The key quantity to study the electron-positron pair production with the QVE is to obtain the momentum distribution function $f(\mathbf{k}, t)$. For spatially homogeneous and time-dependent electric fields, ignoring collisions between particles, the distribution function is determined by $df(\mathbf{k}, t)/dt = S(\mathbf{k}, t)$, where $S(\mathbf{k}, t)$ denotes the source term of pair production. When the strength of the external electric field is relatively large, the induced internal electric field will become significant. So the electric field appearing in the QVE should be the sum of the external and internal electric fields, i.e., $E_{\rm tot}(t) = E_{\rm ext}(t) + E_{\rm int}(t)$. After considering the influence of the backreaction, we can get the coupled equations of the distribution function and the internal electric field

$$\dot{f}(\mathbf{k}, t) = \frac{eE_{\rm tot}(t)\varepsilon_\perp}{2\Omega^2(\mathbf{k}, t)} \int_{-\infty}^{t} dt' \frac{eE_{\rm tot}(t')\varepsilon_\perp}{\Omega^2(\mathbf{k}, t')} [1 - 2f(\mathbf{k}, t')] \times \cos\left[2\int_{t'}^{t} dt'' \Omega(\mathbf{k}, t'')\right], \tag{2}$$

$$\dot{E}_{\rm int}(t) = -4e \int \frac{d^3k}{(2\pi)^3} \left[\frac{k_\parallel(t)}{\Omega(\mathbf{k}, t)} f(\mathbf{k}, t) + \frac{\Omega(\mathbf{k}, t)}{eE_{\rm tot}(t)} \dot{f}(\mathbf{k}, t) - \frac{e\dot{E}_{\rm tot}(t)\varepsilon_\perp^2}{8\Omega^5(\mathbf{k}, t)}\right], \tag{3}$$

where the dot on the letter represents the first-order time derivative, e is the renormalized charge of the electron [23], $\mathbf{k} = (\mathbf{k}_\perp, k_\parallel)$ is the canonical momentum, $k_\parallel(t) = k_\parallel - eA_{\rm tot}(t)$ is defined as the kinetic momentum along the external electric field, $\varepsilon_\perp = \sqrt{m^2 + \mathbf{k}_\perp^2}$ is the transverse energy, m is the mass of the electron, and $\Omega(\mathbf{k}, t) = \sqrt{\varepsilon_\perp^2 + k_\parallel^2(t)}$ is the total energy. The quantum statistics effect and the non-Markov effect on the pair production can be seen from $[1 - 2f(\mathbf{k}, t')]$ in Eq. (2). The first term on the right-hand side of Eq. (3) represents the conduction current, the second term is the polarization current, and the third term is the charge renormalization part added to eliminate the divergence of the polarization current.

For the convenience of numerical calculation, two auxiliary variables $u(\mathbf{k}, t)$ and $v(\mathbf{k}, t)$ are introduced

$$u(\mathbf{k},t) = \int_{-\infty}^{t} dt' W(\mathbf{k},t')[1-2f(\mathbf{k},t')] \times \cos\left[2\int_{t'}^{t} dt''\Omega(\mathbf{k},t'')\right],$$
$$v(\mathbf{k},t) = \int_{-\infty}^{t} dt' W(\mathbf{k},t')[1-2f(\mathbf{k},t')] \times \sin\left[2\int_{t'}^{t} dt''\Omega(\mathbf{k},t'')\right], \tag{4}$$

and then Eq. (2) can be equivalently transformed into the following first-order differential equations

$$\dot{f}(\mathbf{k},t) = \frac{1}{2}W(\mathbf{k},t)u(\mathbf{k},t),$$
$$\dot{u}(\mathbf{k},t) = W(\mathbf{k},t)[1-2f(\mathbf{k},t)] - 2\Omega(\mathbf{k},t)v(\mathbf{k},t),$$
$$\dot{v}(\mathbf{k},t) = 2\Omega(\mathbf{k},t)u(\mathbf{k},t), \tag{5}$$

where $W(\mathbf{k},t) = eE_{\text{tot}}(t)\varepsilon_\perp/\Omega^2(\mathbf{k},t)$.

It can be seen from Eq. (3) that to obtain the internal electric field at time t, the momentum distribution function at the same time must be integrated, but the internal electric field at the same time must be known to calculate the momentum distribution function at time t. To solve this contradiction, we calculate the internal electric field by iteration. First, we use the internal electric field at the previous time $(t-\Delta t)$ to calculate the total electric field at time t by

$$E_{\text{tot}}(t) = E_{\text{ext}}(t) + E^{l}_{\text{int}}(t), \tag{6}$$

where $l = 1, 2, \ldots$ is the number of iterations. Note that for the first iteration $(l = 1)$, the internal electric field $E^1_{\text{int}}(t) = E_{\text{int}}(t-\Delta t)$. Using Eq. (6), the momentum distribution function at time t can be obtained by solving Eq. (5). Then the internal electric field at time t can be solved by Eq. (3). This is the first iteration. Replacing the internal electric field in Eq. (6) with the new one, the second iteration begins. When the internal electric field satisfies our preset control condition $|E^{l+1}_{\text{int}}(t) - E^{l}_{\text{int}}(t)| < \varepsilon$, where ε is a very small number, it can be considered that the real internal electric field at time t has been obtained. Plugging it into the total electric field and solving Eq. (5), the momentum distribution function at time t can be solved as well.

The initial state of the system is a vacuum state without particles, so the single particle distribution function and auxiliary functions satisfy the initial condition $f(\mathbf{k},-\infty) = u(\mathbf{k},-\infty) = v(\mathbf{k},-\infty) = 0$. The initial condition of the internal electric field is $E_{\text{int}}(-\infty) = 0$. After obtaining the single-particle distribution function, integrating it in the full momentum space can obtain the particle number density

$$n(t) = 2\int \frac{d^3k}{(2\pi)^3} f(\mathbf{k},t). \tag{7}$$

The coefficient 2 comes from the spin degeneracy of the fermions.

Note that all our numerical calculations are carried out in the full momentum space. Moreover, before a specific calculation, we demonstrate the reliability of our numerical calculation by comparing our result with that in Ref. [23] and checking the energy conservation of the system when the external electric field is turned off, more details see the Supplemental Material [34].

III. NUMERICAL RESULTS AND ANALYSIS

In this section, we will first study the backreaction effect in the pair production for a rapidly oscillating electric field without frequency chirp (i.e., $b = 0$) in Secs. III A–III C, and then consider it in the pair production for a frequency chirped electric field (i.e., $b \neq 0$) in Sec. III D.

A. Particle number density

In Fig. 1, we show the number density of created particles with (solid black lines) and without (dashed red lines) the backreaction effect for two supercritical electric fields. The field frequencies in Figs. 1(a) and 1(b) are $0.15m$ and $0.35m$, respectively. Other field parameters are $E_0 = 4.0E_{\text{cr}}$ and $\tau = 12.0/m$. It can be seen that the particle number density is invariable when the backreaction is not considered, but the situation is different when the backreaction is considered. For such a supercritical external electric field,

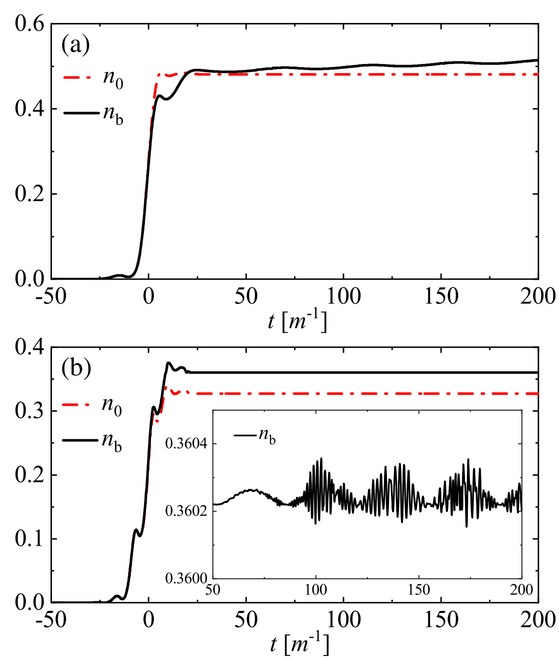

FIG. 1. The particle number density as a function of time with (solid black lines) and without the backreaction (dashed red lines). The external electric field parameters in (a) are $E_0 = 4.0E_{\text{cr}}$, $\omega = 0.15m$, and $\tau = 12.0/m$, and in (b) are $E_0 = 4.0E_{\text{cr}}$, $\omega = 0.35m$, and $\tau = 12.0/m$.

when the field frequency is relatively small, such as $\omega = 0.15m$ in Fig. 1(a), the number density gradually increases with time, which indicates that the internal electric field induces the production of considerable particle pairs. However, when the frequency increases to a certain value, such as $\omega = 0.35m$ in Fig. 1(b), the particle number density remains nearly constant because the internal electric field is not strong enough to stimulate sufficient particle pairs. The reason for the above results is that the electron-positron pairs created in a rapidly oscillating electric field cannot be separated sufficiently by the field to form a strong internal electric field.

In addition, from the inset in Fig. 1(b), one can see that due to the existence of the internal electric field, the particle number density still oscillates with time after the external field vanishes. So it is not easy to obtain a definite particle number density. Fortunately, a recent work [35] shows that the ordinary adiabatic particle number density defined in Eq. (7) can be explained as the number density of physical pairs if the field is switched off immediately at time t. Furthermore, in a wide range of the external field parameters, the oscillation of the number density induced by the internal electric field is very small, for example, see the inset in Fig. 1(b), and the variation range of the number density does not exceed $2.0 \times 10^{-4} m^{-3}$. Therefore, in this case, it is reasonable to choose the number density at any time after the external field entirely disappears as the final number density of created particles. All of our following calculations of the number density are based on the above discussion. Of course, strictly speaking, the number density we calculated is the common adiabatic particle number density or quasiparticle number density.

The particle number density varying with the field frequency for different external electric field amplitudes is shown in Fig. 2. It can be seen that for the subcritical field with $E_0 = 0.1E_{\rm cr}$, see Fig. 2(a), the number density with and without the backreaction effect is almost the same, and the multiphoton absorption is obvious [36]. At the frequency $\omega = 2m/N_0$ with the number of absorbed photons N_0, the particle number density increases greatly. In the figure, $1-, 2-, 3-, 4-$, and $5-$ photon absorption are marked by vertical lines.

However, when $E_0 = 2.0E_{\rm cr}$, $3.0E_{\rm cr}$, and $4.0E_{\rm cr}$, see Fig. 2(b), the multiphoton pair production is not obvious, and simply increasing the frequency of the external field does not enhance the pair production but suppresses it. According to the Keldysh adiabatic parameter [37], $\gamma = m\omega/eE_0$, we can know that in our calculation $\gamma \sim O(1)$. In this range, the tunneling pair production coexists with the multiphoton pair production, and their competitive relation is unfavorable for the pair production. Here it is necessary to give a brief explanation, because, in general, we may think that the pair production should be enhanced by the dynamically assisted mechanism suggested in [10]. However, our study is not belong to this case. First, the dynamically assisted mechanism is achieved by superposing a weak rapidly oscillating field on a strong slowly oscillating field, while we only have a rapidly oscillating electric field here. On a deeper level, when the external field strength exceeds the Schwinger critical field strength, a large number of particles will be created by the tunneling mechanism. Nevertheless, with the increase of the field frequency, more and more particle pairs can be created by absorbing high-frequency photons. This will suppress the pair production dominated by the tunneling mechanism, because the average energy density of the external electric field ($\propto E_0^2$) is fixed for a given field amplitude, and multiphoton pair production spends a part of the electric field energy, but cannot produce a comparable particle number to the tunneling pair production. That is why there is a competitive relation between the tunneling pair production and the multiphoton absorption mechanism, rather than a dynamically assisted mechanism. When $E_0 = 2.0E_{\rm cr}, 3.0E_{\rm cr}$, the backreaction effect is still insignificant, but when $E_0 = 4.0E_{\rm cr}$, the backreaction effect of the internal electric field begins to affect the particle number density; see $\omega \leq 0.85m$.

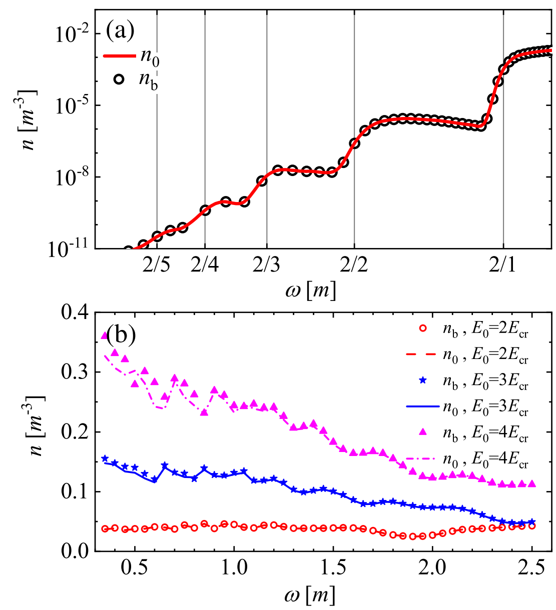

FIG. 2. Particle number density changing with the field frequency for different field amplitudes. In (a), $E_0 = 0.1E_{\rm cr}$, and in (b), $E_0 = 2.0E_{\rm cr}$, $3.0E_{\rm cr}$, $4.0E_{\rm cr}$; the value of τ in both figures is $12.0/m$.

To further investigate the region where the backreaction effect cannot be ignored, we define the difference degree of pair number density (DDOPND) as $\delta = |n_b - n_0|/n_0 \times 100\%$ and study its changes with the external field parameters E_0 and ω; see Fig. 3. Although the supercritical field strength is used in the calculation, which is far away from the current experimental conditions, some interesting results can still be obtained. In our results, for $E_0 \leq 2.0E_{\rm cr}$,

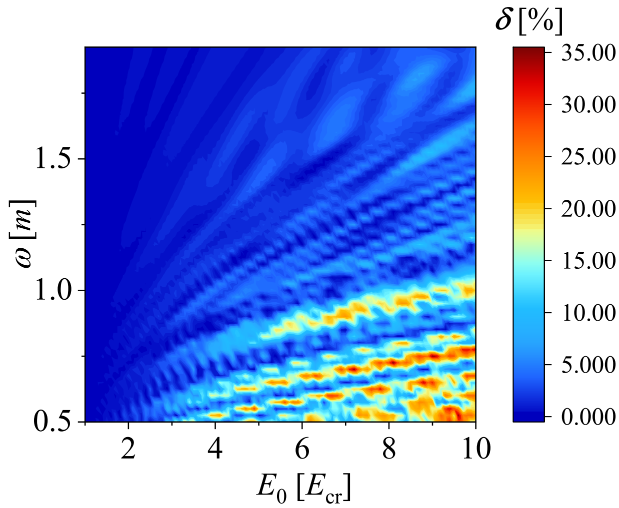

FIG. 3. The difference degree of pair number density (DDOPND) δ as a function of the external field amplitude and frequency. The value of τ in this figure is $12.0/m$. In the calculation, the interval of E_0 is $0.1E_{\mathrm{cr}}$, and the interval of ω is $0.025m$.

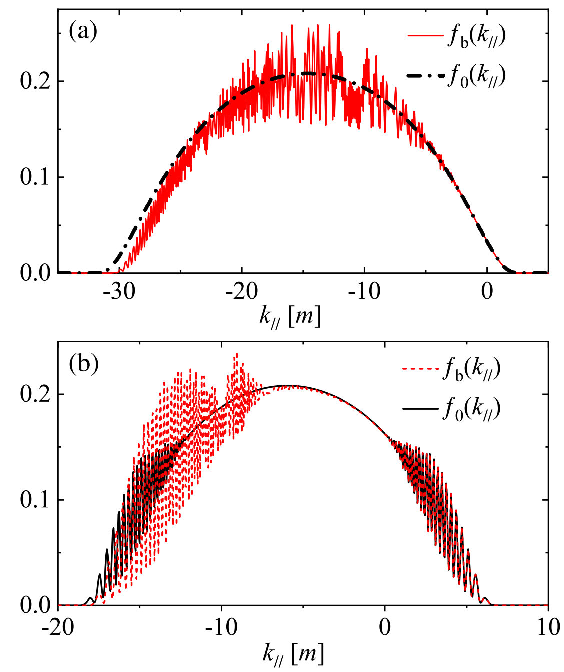

FIG. 4. Comparison of the longitudinal momentum distribution functions between with and without backreaction at $t = 220.0/m$. The transverse momentum $\mathbf{k}_\perp$ is chosen as zero. The parameters of the external electric field in (a) are $E_0 = 2.0E_{\mathrm{cr}}$, $\omega = 0.1m$, $\tau = 12.0/m$, and in (b) are $E_0 = 2.0E_{\mathrm{cr}}$, $\omega = 0.15m$, $\tau = 12.0/m$.

the maximum value of δ is about 1.93% at $E_0 = 2.0E_{cr}, \omega = 0.5m$, and the backreaction effect can be ignored. For $2.0E_{\mathrm{cr}} < E_0 \le 3.0E_{\mathrm{cr}}$, the value of δ is generally within 5%, and in the region where ω is small, the DDOPND value may exceed 5%. When the electric field amplitude E_0 is large and the frequency ω is small, i.e., the Keldysh parameter γ is small, the DDOPND is large, and the backreaction effect is more obvious. In other words, the backreaction effect can generally be neglected in the study of pair production for a weak high-frequency electric field. The reason for this is that the rapid oscillation of the external field is unfavorable for separating the created particle pairs and forming a strong internal electric field. In fact, the change of DDOPND with E_0 and ω is complex. For example, when $E_0 = 7.0E_{\mathrm{cr}}$ and $\omega = 0.8m$, the particle number densities with and without backreaction are about $0.970m^{-3}$ and $0.929m^{-3}$, and $\delta \approx 4.37\%$. The influence of the backreaction effect is almost unnecessary. Whereas, when $E_0 = 7.0E_{\mathrm{cr}}$ and $\omega = 0.9m$, the number densities with and without backreaction are about $0.956m^{-3}$ and $0.773m^{-3}$, and $\delta \approx 23.67\%$. The backreaction effect is very obvious.

B. Momentum spectrum

In Fig. 4, we compare the longitudinal momentum distribution functions of created particles with and without backreaction at $t = 220.0/m$, denoted by f_b and f_0, respectively. The transverse momentum $\mathbf{k}_\perp$ is chosen as zero. Note that the time evolution of the momentum distribution is calculated in the full momentum space. In Fig. 4(a), the momentum distribution f_0 is smooth because the particles are mainly generated by the main peak of the electric field, but the situation is different for slightly larger values of ω. As shown in Fig. 4(b), although the submaximal peak of the electric field cannot produce sufficient particle pairs, the momentum distribution function f_0 shows obvious oscillations because of the infield interference.

Moreover, without the backreaction, the momentum distribution functions f_0 is symmetric about a central longitudinal momentum k_{c} in both cases. This is because the external electric field is an even function of time, and then the total energy satisfies the equation $\Omega(k_\parallel + k_{\mathrm{c}}, -t) = \Omega(-k_\parallel + k_{\mathrm{c}}, t)$. Finally, according to Eq. (2), it can be found that the distribution function satisfies the equation $f_0(k_\parallel + k_{\mathrm{c}}, \infty) = f_0(-k_\parallel + k_{\mathrm{c}}, \infty)$. However, with the backreaction, the symmetry of the momentum distribution function is broken, because the electric field is no longer an even function of time due to the presence of the internal electric field. From the figure, one can also see that there are some irregular oscillations on the momentum spectrum. This embodies a common phenomenon of the backreaction effect rather than numerical errors [22,25,27]. The reason for the presence of the irregular oscillations is that a stochastic process will be developed in the dynamics of vacuum particle production after considering the backreaction effect. For a detailed discussion, see Ref. [25].

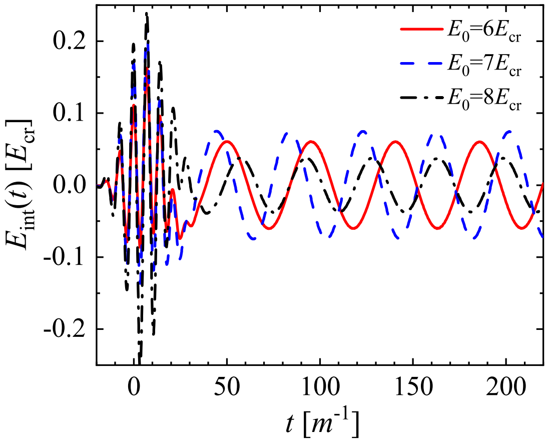

FIG. 5. The internal electric field changes with time for $E_0 = 6.0E_{cr}$, $7.0E_{cr}$, and $8.0E_{cr}$, respectively. Other field parameters are $\omega = 0.9m$ and $\tau = 12.0/m$.

In addition, the backreaction effect is observed in the left side of the momentum spectrum, while on the right side, the momentum spectrum is approximately identical to that without the backreaction effect. Actually, the change of the momentum spectrum with a backreaction effect depends on the time. The position of the backreaction effect on the momentum spectrum oscillates around the central longitudinal momentum with time, because the sign of the induced internal electric field changes with time. A similar phenomenon can be seen in Fig. 4 of Ref. [27].

C. Plasma oscillation period in pair production

We show the time evolution of the internal electric field for different external field amplitudes in Fig. 5. One can see when the external electric field exists ($t < 40/m$), the amplitude of the internal electric field increases with E_0, and its frequency is the same as that of the external electric field. For instance, when $E_0 = 7E_{cr}$, the peak value of the internal electric field is about $0.2E_{cr}$. The motion of particles is mainly dominated by the external electric field. However, when the external electric field is turned off, the relation between the internal electric field and the external field parameters becomes complicated. For example, the amplitude of the internal electric field does not increase monotonically with E_0. And although the external electric field strength is several times the critical electric field strength, when the external electric field vanishes, the induced internal electric field strength is less than $0.1E_{cr}$. This is because the rapid oscillation of the external field makes it difficult to separate the created particle pairs and form a strong internal field.

Moreover, we already know that when the external electric field is strong enough, a large number of electron-positron pairs will be generated, and then when the external electric field vanishes. these particle pairs will maintain a dynamic balance under the action of the internal electric field. Therefore, the motion of the created electron-positron pairs forms plasma oscillation. It is worth noting that the period of plasma oscillation will have some relation with the number density of created particles and the parameters of the external electric field. Previous studies have shown that the frequency of plasma oscillation decreases gradually with time and tends to a stable value at the end [38]. For the external electric field with high intensity and frequency, the frequency of plasma oscillation can reach a stable state quickly.

Assuming that the external electric field disappears at t_0, then the internal electric field at $t > t_0$ can be approximately expressed as

$$E_{int}(t) = E_{int0} \cos\left(\frac{2\pi}{T} t + \varphi\right), \tag{8}$$

where E_{int0} is the amplitude of the internal electric field, T is the period of oscillation, and φ is the phase. In this subsection, we mainly study the relationship between the oscillation period T of the internal electric field and the number density of created particles n by changing the parameters of the external electric field E_0, ω, and τ, respectively.

First, we keep ω and τ unchanged, and E_0 ranges from $5.0E_{cr}$ to $14.0E_{cr}$ with an interval of $1.0E_{cr}$. The oscillation period changing with the particle number density is shown in Fig. 6. The black dots represent the numerical results where the oscillation period of internal electric field T is estimated by Eq. (8). From the results, we can see that the particle number density always increases with the external field amplitude E_0, but the oscillation period T decreases

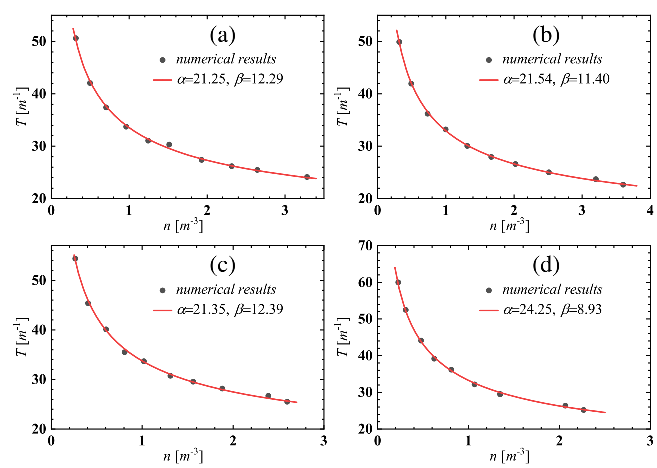

FIG. 6. The oscillation period of electron-positron plasma varying with the particle number density. The ω and τ are fixed and the value of E_0 ranges from $5.0E_{cr}$ to $14.0E_{cr}$ with an interval of $1.0E_{cr}$. Other external electric field parameters are (a) $\omega = 1.5m$, $\tau = 18.0/m$; (b) $\omega = 1.5m$, $\tau = 30.0/m$; (c) $\omega = 1.7m$, $\tau = 12.0/m$; (d) $\omega = 2.0m$, $\tau = 12.0/m$.

TABLE I. The 95% confidence intervals for fitting parameters α and β in Fig. 6. The square brackets indicate the lower and upper limits of the interval.

	α	β
(a)	[20.50, 22.00]	[11.52, 13.07]
(b)	[21.13, 21.94]	[10.99, 11.81]
(c)	[20.59, 22.11]	[11.53, 13.25]
(d)	[23.68, 24.82]	[8.21, 9.65]

with the increase of the number density. The red lines are the fitting curves corresponding to the fitting formula

$$T(n) = \frac{\alpha}{\sqrt{n}} + \beta, \tag{9}$$

where n is the particle number density, and α and β are fitting parameters. Note that this formula is constructed based on the frequency of Langmuir oscillation [39] in plasma physics. Although it is a little different from the ultrarelativistic formula given in Ref. [24], both of them have the same varying tendency. In Figs. 6(a)–6(d), the goodness of fit R^2 is about 0.998, 0.999, 0.998, and 0.999, respectively. The 95.0% confidence intervals for fitting parameters α and β are shown in Table I. This shows that the formula above can fit the numerical results very well.

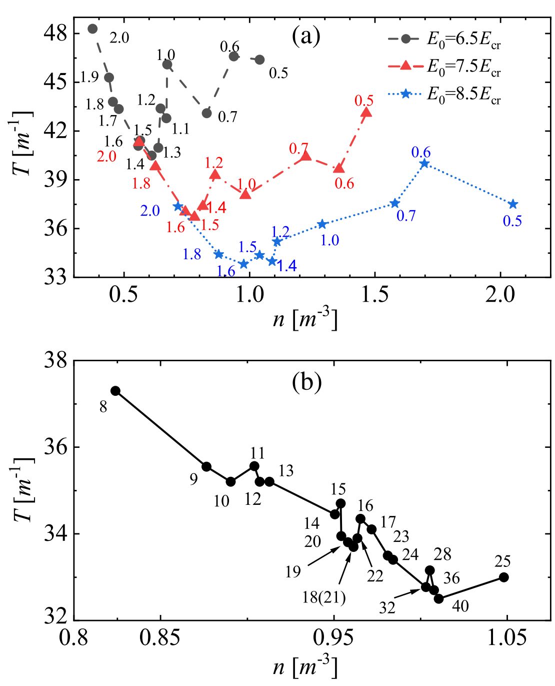

FIG. 7. The oscillation period of electron-positron plasma varying with the particle number density. In (a), $E_0 = 6.5E_{\mathrm{cr}}$, $7.5E_{\mathrm{cr}}$, $8.5E_{\mathrm{cr}}$, and $\tau = 12.0/m$ are fixed, and ω ranges from $0.5m$ to $2.0m$. The particle number density changes with ω. In (b), $E_0 = 8.0E_{\mathrm{cr}}$ and $\omega = 1.5m$ are constant, and the particle number density changes with τ.

Furthermore, since the fitting parameters α and β are almost independent of E_0, the oscillation period T is not directly related to E_0. Finally, we emphasize that the external electric field we considered here is a high-frequency strong field. For other cases, the fitting formula (9) may fail.

When E_0 and τ are kept unchanged while ω is changing, or when E_0 and ω are kept constant and τ is changing, the above fitting formula will be invalid; see Fig. 7. The relation between the oscillation period and the number density of created pairs is very complex and not monotonically decreasing. In Fig. 7(a), we change the value of ω and mark each data point with the frequency of the external electric field. It can be seen that the particle number density generally decreases with the increase of the frequency ω. In the high-frequency region, such as $\omega \geq 1.6m$ for $E_0 = 6.5E_{\mathrm{cr}}$, $\omega \geq 1.5m$ for $E_0 = 7.5E_{\mathrm{cr}}$, and $\omega \geq 1.6m$ for $E_0 = 8.5E_{\mathrm{cr}}$, the oscillation period decreases with the increase of particle number density. This behavior is somewhat similar to that in Fig. 6. But when the frequency takes other values, the relation between them exhibits very complex oscillations. In particular, we find that in the low frequency region (such as $\omega = 0.6m$), the fitting formula (9) still fails even if the field frequency and the pulse duration are fixed, and only the field amplitude changes, because the number density does not decrease monotonically with the field amplitude. In Fig. 7(b), we change the value of τ and mark each data point with the value of τ. It can be seen that the relation between the particle number density and the pulse duration τ is not monotonic. As the pulse duration increases, the number density of created pairs may not increase. Thus, the fitting formula (9) also does not work here. In addition, from Fig. 7(a), we can see that for $E_0 = 6.5E_{\mathrm{cr}}$, the number density of created particles at $\omega = 1.1m$ almost equals that at $\omega = 1.0m$, but their oscillation periods have a big difference. That is to say, the particle number density for different field frequencies can be equal, see Fig. 2, but the same number density corresponds to different oscillation periods. This shows that the oscillation periods directly depend on not only the particle number density but also the field frequency. Similarly, from Fig. 7(b), we can find that the oscillation periods also directly depend on the pulse duration, because the different number density corresponding to different pulse durations gives the same oscillation period; see the data points marked with the pulse duration of 12 and 13.

We further explore the relation between the oscillation period and the particle number density for fixing $E_0 = 7.0E_{\mathrm{cr}}$ and keeping $\omega\tau = 20.0$, which ensures that the number of cycles in the external electric field is constant; see Fig. 8. To separate the number density, the value of ω ranges from $0.4m$ to $1.65m$ with a variable interval. In the figure, each data point is marked with the corresponding frequency value. From the figure, we find that with the frequency increasing (the pulse duration decreasing

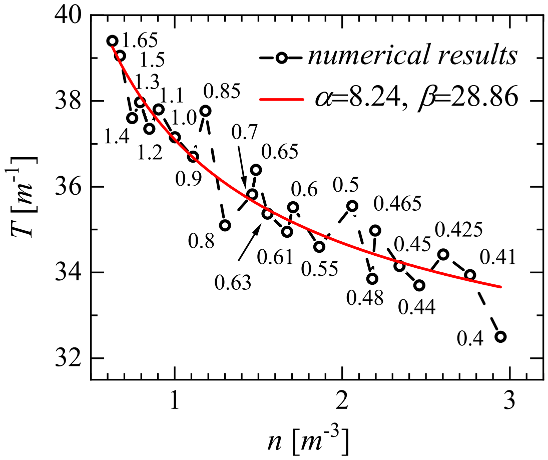

FIG. 8. The oscillation period of electron-positron plasma changing with the particle number density. Here $E_0 = 7.0E_{\mathrm{cr}}$, $\omega\tau = 20.0$ is kept to ensure that the number of cycles in the external electric field is constant. The value of ω ranges from $0.4m$ to $1.65m$ and τ changes accordingly.

correspondingly), the particle number density always decreases. When the value of ω is relatively small, the particle number density changes rapidly with ω. For example, when ω changes from $0.41m$ to $0.4m$, the particle number density changes by $0.1817m^{-3}$, while when ω changes from $1.5m$ to $1.4m$, the number density only changes by $0.0725m^{-3}$. This result is also reflected in Fig. 4(a). Besides this, the oscillation period tends to decrease with the increase of the number density. Therefore, we can try to fit it with Eq. (9). The fitted curve is represented by the solid red line in Fig. 8, and the goodness of fit R^2 is about 0.89. The 95.0% confidence intervals for α and β are [6.99, 9.49] and [27.76, 29.96], respectively. This suggests that considering the product of ω and τ as a whole may be more helpful to explore the relation between the oscillation period and the number density of produced pairs.

It is noted that the approximate expression of the internal electric field Eq. (8) is obtained under the premise that the external field is zero, but the plasma oscillation period is still directly related to the external field parameters E_0, ω, and τ, which also embodies the non-Markov effect in the electron-positron pair production.

D. Backreaction effect in pair production for a frequency chirped electric field

From Eq. (1), it can be seen that the external electric field will be modulated by a linear frequency chirp when the chirp parameter b is nonzero. Furthermore, the oscillation frequency of the external field is smaller than ω at $-2\omega/b < t < 0$ for $b > 0$ and $0 < t < -2\omega/b$ for $b < 0$, while it is greater than or equal to ω when t is beyond the above range. So the slowly oscillating part of the external field appears at $t < 0$ for a positive chirp parameter, and at $t > 0$ for a negative chirp parameter. Below we will explore the beakreaction effect in pair production for different frequency chirped electric fields.

In our previous work [18], it was found that the particle number density would be significantly increased by introducing the frequency chirp. For instance, the number density can be enhanced by 4 orders of magnitude for a linearly polarized electric field with the field parameters $E_0 = 0.1\sqrt{2}E_{\mathrm{cr}}$, $\omega = 0.6m$, $\tau = 10.0/m$, and $b = 0.06m^2$. To check whether the backreaction effect should be considered, we calculate the time evolution of the particle number density with and without the backreaction and the induced internal electric fields for the chirp parameter $b = 0$ (red lines), $0.06m^2$ (black lines), $-0.06m^2$ (blue lines); see Fig. 9. First, it can be seen that although the intermediate values of the number density for the positive and the negative chirp are different in the absence of the backreaction effect, their final number density is the same; see Figs. 9(a), 9(c), and 9(e). This result reproduces our findings in Ref. [40]; i.e., the pair production triggered by a spatially homogeneous and frequency chirped electric field is remarkably immune to the temporal phase information contained in the field because of the time reversal symmetry between the positive and the negative chirped fields. However, this immunity is destroyed after considering the backreaction effect, because the induced internal fields break the time reversal symmetry between these two chirped fields; see Figs. 9(b), 9(d), and 9(f).

In addition, from Fig. 9(a), we find that for a subcritical electric field, although the number density is enhanced by 4 orders of magnitude after introducing a linear frequency chirp, the backreaction effect can still be neglected. Furthermore, the backreaction is still insignificant even for a supercritical field whose field amplitude has reached $2.0E_{\mathrm{cr}}$; see Fig. 9(c). This result indicates that regardless of whether the rapidly oscillating subcritical electric field has a frequency chirp or not, the backreaction effect in this case is negligible.

In order to understand the above result, we turn to analyzing the induced internal electric fields changing with time for different chirp parameters. In previous sections, we have found that the faster the oscillation of the external field, the more difficult it is to achieve charge separation and form a strong internal electric field. However, the situation is more complicated for a frequency-chirped electric field, because the field consists of two rapidly oscillating parts and a slowly varying part, and the latter one is between the former two. Moreover, particle pairs are easily produced at the rapidly oscillating part while they are easy to form a charge separation at the slowly varying part. So we previously speculated that a stronger internal electric field may be induced in pair production for a frequency-chirped electric field. This speculation is well demonstrated in Figs. 9(b), 9(d), and 9(f). From these figures, one can see that the internal electric field for a chirped field is much

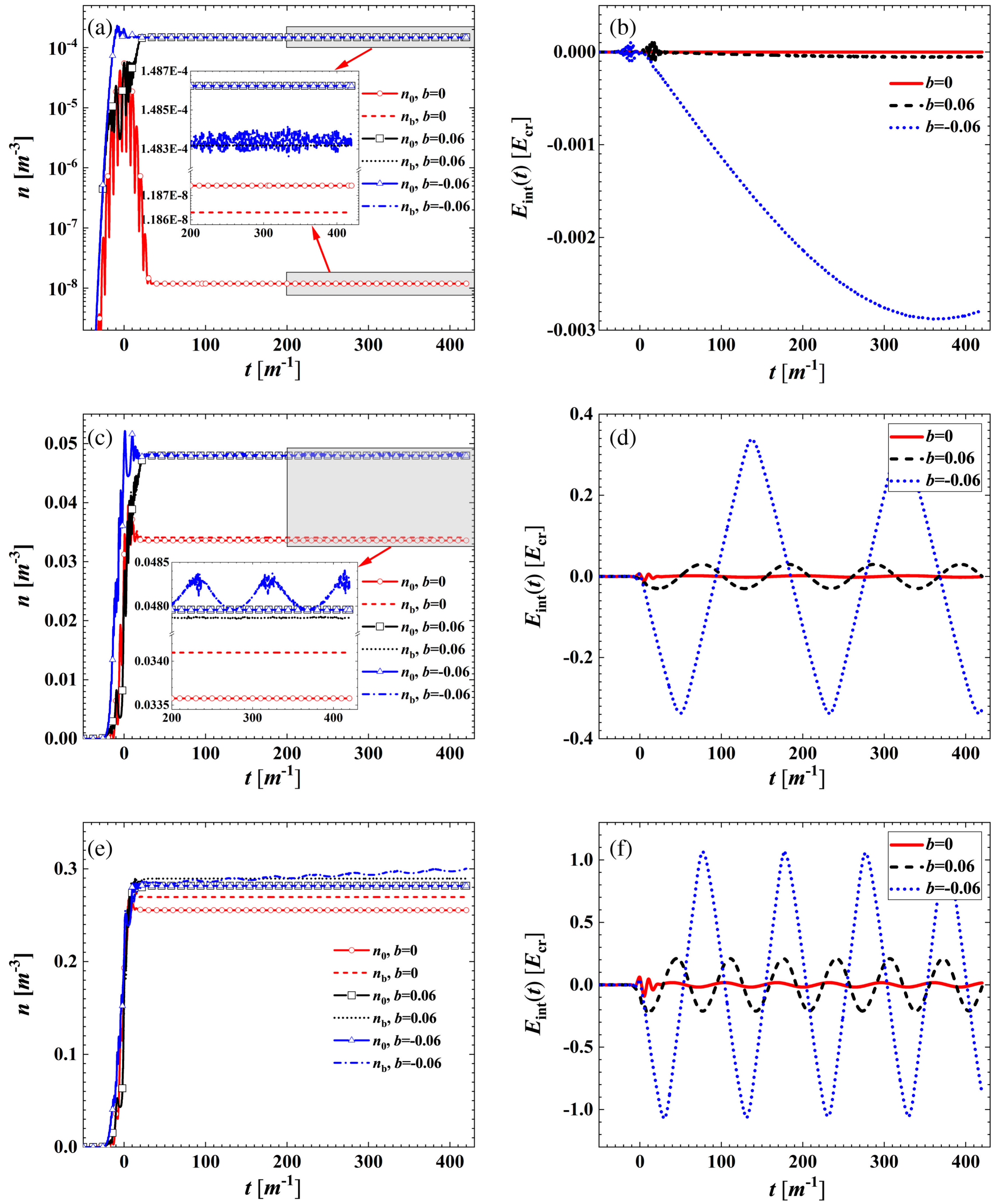

FIG. 9. The time evolution of the particle number density with and without backreaction (see (a), (c), and (e)) and the induced internal electric fields (see (b), (d), and (f)) for the chirp parameter $b = 0, 0.06m^2, -0.06m^2$. The amplitudes of external electric fields are $0.1\sqrt{2}E_{cr}$ (see (a) and (b)), $2.0E_{cr}$ (see (c) and (d)), $4.0E_{cr}$ (see (e) and (f)), respectively. Other external electric field parameters are $\omega = 0.6m$ and $\tau = 10.0/m$.

stronger than that for an unchirped field. Also, the internal electric field for a negative chirp is much stronger than that for a positive chirp. That is because in the case of a negative chirp, more particles are produced at $t < 0$ and then achieve a better charge separation at $0 < t < -2\omega/b$, while for the positive chirp, the charge separation has finished at $-2\omega/b < t < 0$ before more particles are produced at $t > 0$. Even so, from Figs. 9(b) and 9(d), we can see that the induced internal electric field for a chirped field is still much weaker than the external electric field. Therefore, the effect of the internal electric field on the particle number density is insignificant for a weak rapidly oscillating electric field with or without a frequency chirp. Of course, when the external field becomes sufficiently strong, the induced internal electric field may have a non-negligible impact on the external field, and the backreaction effect can no longer be ignored. Particularly, when the induced internal electric field is stronger than the critical field after the external field disappeared, a large number of particle pairs are still being produced in the internal field, and the backreaction effect will become increasingly evident; see the case of $b = -0.06m^2$ in Figs. 9(e) and 9(f). Note that the effect of the induced internal electric field on the external one is also related to the relative phase between them. For instance, in Figs. 9(e) and 9(f), the backreaction effect for $b = 0$ is more obvious than that for $b = 0.06m^2$ because the internal field oscillates roughly in phase with the external field for the former one.

IV. SUMMARY AND DISCUSSION

In summary, the backreaction effect and plasma oscillation in the pair production for a rapidly oscillating electric field are investigated by the QVE approach.

First, the parameter region of the external electric field where the backreaction effect cannot be ignored is explored by calculating and analyzing the difference degree of pair number density with and without the backreaction. It is found that the backreaction effect can be neglected in the pair production for a weak rapidly oscillating electric field with or without a frequency chirp. In particular, the backreaction effect can be ignored in the pair production for a subcritical external field with frequency chirp. This result is beyond what we previously thought, because the great improvement of particle number density by absorbing some high-frequency photons is expected to obtain a good charge separation by the slowly varying part of the external field, and form a strong internal electric field, which makes the backreaction effect become obvious. The reason for this is that although in some regions, the particle number density can be greatly improved by increasing the field frequency, the rapid oscillation generally is unfavorable for separating the created particle pairs and form a strong internal electric field. Thus, to study the backreaction effect, the external electric field strength should be larger than the critical one. However, for a strong high-frequency electric field, the pair production is dominated by tunneling pair production and the multiphoton absorption mechanism at the same time, which will suppress the pair production because of the competitive relation between these two mechanisms.

The influence of the backreaction effect on the momentum spectrum is also considered. It is found that after considering the backreaction effect, the symmetry of the momentum spectrum is broken, and some irregular oscillations are observed on the momentum spectrum.

Finally, the relationship between the plasma oscillation period and the number density of produced particle pairs is studied. When the frequency and duration of the external electric field are kept constant and only the field strength is changed, the relation between the oscillation period and the particle number density is obvious and can be fitted by a simple formula constructed based on the Langmuir oscillation frequency. However, when the field frequency or the pulse duration changes, the relationship between the oscillation period and the particle number density is very complex. One way to ensure that the oscillation period is regular is to keep the number of cycles in the external electric field unchanged when changing the field frequency. Furthermore, we find that the plasma oscillation period not only directly depends on the final number density of created particles, but also directly depends on the external field parameters, such as the field strength, the field frequency, and the pulse duration, which is different from the common result in plasma physics. The reason for this is that the external electric field has left an imprint on the internal field by the non-Markov effect in pair production.

Our results clarify the question whether it is reasonable to study the pair production for a subcritical electric field with frequency chirp and deepen the understanding of the factors influencing the plasma oscillation period.

ACKNOWLEDGMENTS

The work is supported by the National Natural Science Foundation of China (NSFC) under Grants No. 11974419, No. 12304337, and No. 11705278, and by the Fundamental Research Funds for the Central Universities (No. 20226943 and No. 2023ZKPYL02).

[1] P. A. M. Dirac, The quantum theory of the electron, Proc. R. Soc. A **117**, 610 (1928).
[2] F. Sauter, Über das Verhalten eines Elektrons im homogenen elektrischen Feld nach der relativistischen Theorie Diracs, Z. Phys. **69**, 742 (1931).
[3] J. Schwinger, On gauge invariance and vacuum polarization, Phys. Rev. **82**, 664 (1951).
[4] B. S. Xie, Z. L. Li, and S. Tang, Electron-positron pair production in ultrastrong laser fields, Matter Radiat. Extremes **2**, 225 (2017).
[5] A. Fedotov, A. Ilderton, F. Karbstein, B. King, D. Seipt, H. Taya, and G. Torgrimsson, Advances in QED with intense background fields, Phys. Rep. **1010**, 1 (2023).

[6] K. A. Tanaka *et al.*, Current status and highlights of the ELI-NP research program, Matter Radiat. Extremes **5**, 024402 (2019).

[7] G. Tiwari, E. Gaul, M. Martinez, G. Dyer, J. Gordon, M. Spinks, T. Toncian, B. Bowers, X. Jiao, R. Kupfer, L. Lisi, E. McCary, R. Roycroft, A. Yandow, G. D. Glenn, M. Donovan, T. Ditmire, and B. M. Hegelich, Beam distortion effects upon focusing an ultrashort petawatt laser pulse to greater than 10^{22} W/cm^2, Opt. Lett. **44**, 2764 (2019).

[8] J. W. Yoon, Y. G. Kim, I. W. Choi, J. H. Sung, H. W. Lee, S. K. Lee, and C. H. Nam, Realization of laser intensity over 10^{23} W/cm^2, Optica **8**, 630 (2021).

[9] A. Ringwald, Pair production from vacuum at the focus of an X-ray free electron laser, Phys. Lett. B **510**, 107 (2001). European XFEL: https://www.xfel.eu/. ELI: https://www.eli-beams.eu/.

[10] R. Schützhold, H. Gies, and G. Dunne, Dynamically assisted Schwinger mechanism, Phys. Rev. Lett. **101**, 130404 (2008).

[11] A. Nuriman, B. S. Xie, Z. L. Li, and D. Sayipjamal, Enhanced electron-positron pair creation by dynamically assisted combinational fields, Phys. Lett. B **717**, 465 (2012).

[12] C. Fey and R. Schützhold, Momentum dependence in the dynamically assisted Sauter-Schwinger effect, Phys. Rev. D **85**, 025004 (2012).

[13] C. Kohlfürst, M. Mitter, G. von Winckel, F. Hebenstreit, and R. Alkofer, Optimizing the pulse shape for Schwinger pair production, Phys. Rev. D **88**, 045028 (2013).

[14] Z. L. Li, D. Lu, B. S. Xie, L. B. Fu, J. Liu, and B. F. Shen, Enhanced pair production in strong fields by multiple-slit interference effect with dynamically assisted Schwinger mechanism, Phys. Rev. D **89**, 093011 (2014).

[15] M. Jiang, B. S. Xie, H. B. Sang, and Z. L. Li, Enhanced electron-positron pair creation by the frequency chirped laser pulse, Chin. Phys. B **22**, 100307 (2013).

[16] N. Abdukerim, Z. L. Li, and B. S. Xie, Enhanced electron-positron pair production by frequency chirping in one- and two-color laser pulse fields, Chin. Phys. B **26**, 020301 (2017).

[17] C. Gong, Z. L. Li, B. S. Xie, and Y. J. Li, Electron-positron pair production in frequency modulated laser fields, Phys. Rev. D **101**, 016008 (2020).

[18] O. Olugh, Z. L. Li, B. S. Xie, and R. Alkofer, Pair production in differently polarized electric fields with frequency chirps, Phys. Rev. D **99**, 036003 (2019).

[19] K. Wang, X. Hu, S. Dulat, and B. S. Xie, Effect of symmetrical frequency chirp on pair production, Chin. Phys. B **30**, 060204 (2021).

[20] L. J. Li, M. Mohamedsedik, and B. S. Xie, Enhanced dynamically assisted pair production in spatial inhomogeneous electric fields with the frequency chirping, Phys. Rev. D **104**, 036015 (2021).

[21] M. Mohamedsedik, L. J. Li, and B. S. Xie, Schwinger pair production in inhomogeneous electric fields with symmetrical frequency chirp, Phys. Rev. D **104**, 016009 (2021).

[22] Y. Kluger, J. M. Eisenberg, B. Svetitsky, F. Cooper, and E. Mottola, Fermion pair production in a strong electric field, Phys. Rev. D **45**, 4659 (1992).

[23] J. C. R. Bloch, V. A. Mizerny, A. V. Prozorkevich, C. D. Roberts, S. M. Schmidt, S. A. Smolyansky, and D. V. Vinnik, Pair creation: Back reactions and damping, Phys. Rev. D **60**, 116011 (1999).

[24] R. Alkofer, M. B. Hecht, C. D. Roberts, S. M. Schmidt, and D. V. Vinnik, Pair creation and an x-ray free electron laser, Phys. Rev. Lett. **87**, 193902 (2001).

[25] D. V. Vinnik, V. A. Mizerny, A. V. Prozorkevich, S. A. Smolyansky, and V. D. Toneev, Kinetic description of vacuum particle production in collisions of ultrarelativistic nuclei, Phys. At. Nucl. **64**, 775 (2001).

[26] C. D. Roberts, S. M. Schmidt, and D. V. Vinnik, Quantum effects with an x-ray free-electron laser, Phys. Rev. Lett. **89**, 153901 (2002).

[27] B. Mihaila, J. F. Dawson, and F. Cooper, Fermion pair production in QED and the backreaction problem in $(1+1)$-dimensional boost-invariant coordinates revisited, Phys. Rev. D **78**, 116017 (2008).

[28] S. Pla, I. M. Newsome, R. S. Link, P. R. Anderson, and J. Navarro-Salas, Pair production due to an electric field in $1+1$ dimensions and the validity of the semiclassical approximation, Phys. Rev. D **103**, 105003 (2021).

[29] F. Hebenstreit, J. Berges, and D. Gelfand, Simulating fermion production in $1+1$ dimensional QED, Phys. Rev. D **87**, 105006 (2013).

[30] F. Hebenstreit, J. Berges, and D. Gelfand, Real-time dynamics of string breaking, Phys. Rev. Lett. **111**, 201601 (2013).

[31] Q. Z. Lv, S. Dong, Y. T. Li, Z. M. Sheng, Q. Su, and R. Grobe, Role of the spatial inhomogeneity on the laser-induced vacuum decay, Phys. Rev. A **97**, 022515 (2018).

[32] C. Kohlfürst, Effect of time-dependent inhomogeneous magnetic fields on the particle momentum spectrum in electron-positron pair production, Phys. Rev. D **101**, 096003 (2020).

[33] C. Kohlfürst, N. Ahmadiniaz, J. Oertel, and R. Schützhold, Sauter-Schwinger effect for colliding laser pulses, Phys. Rev. Lett. **129**, 241801 (2022).

[34] See Supplementary Material at http://link.aps.org/supplemental/10.1103/PhysRevD.108.076015 for more details, which includes Refs. [23,25,29].

[35] A. Ilderton, Physics of adiabatic particle number in the Schwinger effect, Phys. Rev. D **105**, 016021 (2022).

[36] C. Kohlfürst, H. Gies, and R. Alkofer, Effective mass signatures in multiphoton pair production, Phys. Rev. Lett. **112**, 050402 (2014).

[37] L. V. Keldysh, Ionization in the field of a strong electromagnetic wave, Sov. Phys. JETP **20**, 1307 (1965).

[38] A. Benedetti, W. B. Han, R. Ruffini, and G. V. Vereshchagin, On the frequency of oscillations in the pair plasma generated by a strong electric field, Phys. Lett. B **698**, 75 (2011).

[39] L. Tonks and I. Langmuir, Oscillations in ionized gases, Phys. Rev. **33**, 195 (1929).

[40] C. Gong, A. Penwell, Z. L. Li, Y. J. Li, Q. Su, and R. Grobe, Transition between coherent and incoherent chirping mechanisms in electron-positron pair creation, J. Opt. Soc. Am. B **37**, 1098 (2020).